Journal of Sol-Gel Science and Technology (2024) 110:792–806
https://doi.org/10.1007/s10971-024-06385-x

ORIGINAL PAPER

Impact of electron–hole recombination mechanism on the photocatalytic performance of ZnO in water treatment: A review

Alaa Nihad Tuama[1] · Laith H. Alzubaidi[2] · Muhammad Hasnain Jameel[3] · Khalid Haneen Abass[1] · Mohd Zul Hilmi bin Mayzan[3] · Zahraa N. Salman[4]

Received: 1 March 2024 / Accepted: 8 April 2024 / Published online: 14 May 2024

Abstract

One of the most popular standard benchmark photocatalysts in the water treatment and environmental applications fields is zinc oxide (ZnO). Nevertheless, the total photocatalytic efficacy is limited by ZnO's high band gap and the significant recombination of photogenerated charge carriers, particularly in its nano size. This can be further circumvented by hybridizing ZnO with a material that has a narrow band gap, such as metallic, non-metallic, carbon-based, or polymeric-based, to change its electronic band structure and other pertinent features. The use of ZnO-based photocatalyst in wastewater treatment shows a lot of potential as an effective and long-lasting oxidation technique. To increase photocatalytic efficiency, ZnO photocatalysts can be prepared in a variety of ways and modified via doping. In the present review, we assess recent studies on the creation of ZnO-based photocatalysts for the treatment of water using a variety of preparation methods based on electron–hole generation and recombination. The majority of development strategies and research on attaining the best possible photocatalysis performance in high-yield degradation with related factors are discussed, and the primary reasons for increased efficiency are explained. We consider areas where ZnO-based photocatalysts for water treatment could be improved. Finally, there is also a discussion of the prospects and challenges in this exciting field. Our evaluation aims to assist researchers in creating photocatalysts for water treatment that are both affordable and highly effective.

Graphical Abstract

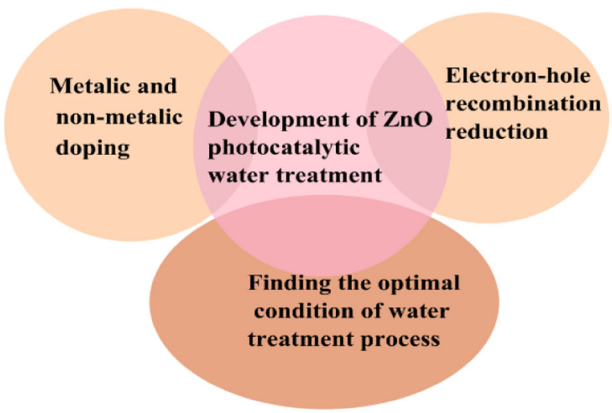

✉ Alaa Nihad Tuama
Pure.alaa.tuama@uobabylon.edu.iq

[1] Department of Physics, College of Education for Pure Sciences, University of Babylon, Hillah, 5001 Hillah, Iraq

[2] Department of Computers Techniques Engineering, College of Technical Engineering, The Islamic University, Najaf, Iraq

[3] Department of Physics, Faculty of Applied Sciences and Technology, Universiti Tun Hussein Onn Malaysia, 84600 Pagoh, Johor, Malaysia

[4] Medical Physics Department, Hilla University College, Babylon, Iraq

Keywords: Electron–hole recombination · Photocatalytic performance · Zn · Water treatment · Metallic and non-metallic doping

Highlights

- A variety of preparation techniques have been used to employ metallic and non-metallic doped zinc oxide (ZnO) based photocatalysts broadly in the field of water treatment.
- Total photocatalytic efficacy is limited by ZnO's high band gap and the significant recombination of photogenerated charge carriers, particularly in its nano size.
- Harmful organic and inorganic contamination in water can likely be resolved by adjusting the initial pollutant level, pH, and intensity of light.
- Hybridizing ZnO with a material that has a narrow band gap, such as metallic, non-metallic, carbon-based, or polymeric-based, to change its electronic band structure and other pertinent features.

1 Introduction

One of the main environmental challenges associated with the present worldwide crisis is the pollution of natural water sources with hazardous organic chemical substances, such as organic dyes and insecticides released as effluents of wastewater from industry testing facilities and local agriculture, respectively. In addition to the impacts caused by human activity, a lack of clean water resources will likely be a problem for humanity due to changes in the climate and warming temperatures. For these reasons, major communities must demand the recycling and purification of spent water. Reverse osmosis, electrodialysis, gas stripping, and heterogeneous photocatalysis are just a few water treatment techniques that emerged over the years [1–7]. Continuous development of pure and heterogeneous photocatalysis for the treatment of water has been conducted. The technique of heterogeneous photocatalysis has great potential and is useful for both environmental and energy applications. Due to its benefits, including affordability, non-toxicity, complete mineralization, and reusability, it has developed into a rapidly expanding field of study over the past few decades. The following noteworthy semiconductors have been used as photocatalysts: CdO, TiO_2, ZnO, ZnS, WO_3, and CdTe [8].

Due to their electrical band structures, the materials described above, the two metal oxides that are most frequently used as photocatalysts are ZnO in the wurtzite phase and TiO2 in anatase form. In recognition of its higher quantum efficiency, ZnO is thought to operate photocatalytically more effectively than TiO_2 in many circumstances [9, 10]. ZnO nanostructures are a wide band gap (Eg) semiconductor with a band gap of 3.37 eV. However, an intrinsic limitation prevents them from using about 4% of the UV component of solar light as a consistent, plentiful, and aesthetically pleasing source of energy for photoexcitation during the reaction. Consequently, a significant amount of research has been done to expand ZnO's photoresponse into the visible light area (about 43% of the solar spectrum) [11]. One of the primary tactics is to modify the ZnO band structure to the reduced band gap to customize visible-light absorption. Several strategies and tactics were used and documented to accomplish this significant objective. We shall allude to these efforts in this review.

It is well known that adding metals and nonmetals to the ZnO structure results in a red shift in the band gap, which creates visible light-active photo-catalysts [12]. With no modifications to the band gap, metal doping in the first example creates shallow- or deep-level states that can absorb longer wavelength light absorption. These intra-band states acting as a recombination center may decrease the photocatalytic performance. When dopants are incorporated into the band gap in the nonmetal doping scenario, local states are created inside the gap, allowing ZnO's absorption initiation to be prolonged from the UV to the visible light range by band gap reduction [13]. Numerous research conducted to date has shown that metal-doped ZnO (Cu, Mn, Ag, Fe, Co, Eu, Al, and Ce) and nonmetal-doped ZnO (C, N, and S) cause the optical absorption edge of ZnO to redshift to lower energies and enhanced photocatalytic activity in the visible light domain as demonstrated in Table 1. Table 1 provides an overview of the most often used dopants in ZnO structure, synthesis methods, and experimental configurations for visible-light photocatalytic applications on water treatment.

Generally, quasi-stable energy states inside the band gap energy are produced by doping appropriate metal oxides with transition metals. Additionally, adding the right amount of ions to the host lattice will enhance electron trapping because of the increased surface sites, and the change in band gap energy (Eg) would boost photocatalytic efficiency. The decreased rate of electron–hole pair recombination makes this possible [14]. Consequently, a novel ternary nanocomposite has been widely developed between the metal oxides of ZnO and different dopant materials as previously discussed to reduce photoinduced

Table 1 A synopsis of the most prevalent dopants in ZnO nanostructures, accompanied by details of their synthesis procedures and photocatalytic operational parameters

Doping	Precursor of doping	Technique of synthesis	Contaminant	Source	Photocatalytic circumstances	Ref
Al	$AlCl_3{\cdot}6H2O$	Sol–gel	Rhodamine 6G (R6G)	Tungsten lamp 200 W	3.5 cm^2 of photocatalyst and 100 ml of 10–5 M R6G	[78]
Cu	$Cu(CH_3COO)_2$	Co-precipitation	Crystal violet (CV)	Mercury- lamp	0.25 g of photocatalyst, 100 ml of 10 mg/L CV	[79]
Fe	$Fe(NO_3)3{\cdot}9H_2O$	Hydrothermal	Rhodamine B (RB)	Xenon lamp with 500 W	20 mg of photocatalyst, 20 mL of 10 mg/L RhB	[80]
Ag	$AgNO_3$	Sol–gel	Methylene blue	Fluorescent tubes with 15 W	150 mL of 10–5 M MB, 150 mg of photocatalyst	[81]
Mn	$MnSO4{\cdot}H2O$, 99%	Echo-green route	Methylene blue	UV light with 30 W	100 mL of MB, 100 mg of photocatalyst	[82]
Mn	$MnCl_2$	Wet-chemical	Rhodamine B	Xenon lamp300 W	40 mg of photocatalyst, 100 ml of 10–5 M RB,	[83]
Co	$CoCl2{\cdot}6H2O$	Wet-chemical	Methylene blue	Sunlight (natural)	5 mg of photocatalyst, 10^{-6} M of MB	[84]
Ce	Cerium acetate hydrate(III)	Hydrothermal	Acetaldehyde	LED (Blue)	Photocatalyst (0.1 g)	[85]
Eu	$Eu(Cl)3{\cdot}6H2O$	Wet-chemical	Phenol	Sunlight (natural)	100 mg of photocatalyst, 100 mL of 20 mg/L phenol	[86]
N	Urea	Sol–gel	Picloram, 2, 4-D	Tungsten–halogen lamp(25 W)	20 mg L − 1 of 2,4-D	[87]
C	MWCNT	Electrospinning	Methylene blue	Solar simulator	10 mg of photocatalyst, 20 mL of 10–5 M MB	[88]
C	$C_4H6O_4Zn{\cdot}2H_2O$, 99.0%	Electrospinning	Carbon dioxide	Solar Xe arc lamp (350 W)	100 ml of CO_2	[89]
Ni	$NiCl_2{\cdot}6H_2O$	Solvo-thermal	Methylene blue	15 W UV light	30 mg of photocatalyst, 100 mL of MB	[90]

electron–hole recombination by promoting electrical conductivity, charge circulation, and light absorption process which can be invested to improve the water-treatment and photocatalytic properties of ZnO. ZnO has drawn much interest for its ability to fully mineralize and degrade pollutants in the environment. ZnO's photocatalytic performance is expected to be comparable to TiO2's because of their almost identical band gap energies (3.2 eV). Furthermore, ZnO is comparatively less expensive than TiO2, while TiO2 is not cost-effective for use in large-scale water treatment processes. ZnO is an essential photocatalyst in environmental and water treatment because of its largest advantage: it can absorb a greater range of the solar spectrum and more light quanta than certain semiconducting metal oxides [15–17].

In this study, we offer a new-era perspective on the development of both substituted ZnO and pure nanomaterials using various materials and methods to enhance photocatalytic activity. Metal doping, nonmetal doping, rare-earth metal doping, and other metal doping will be compared and analyzed in the context of minimizing electron–hole recombination.

2 The basics of ZnO

ZnO is an II–VI oxide semiconductor that has a significant exciton binding energy of 60 meV at ambient temperature and a direct large band gap of 3.37 eV. ZnO nanomaterials are the best option for optoelectronic and electronic applications such as diodes (LEDs), sensors, actuators, field-emission devices, UV laser diodes, solar cells, spintronic, piezoelectric, and photocatalysts devices because of their outstanding piezoelectric and optoelectronic characteristics, biological compatibility, benign nature, and thermal resilience [18]. Because of its distinctive properties, zinc oxide (ZnO) has emerged as the front-runner in photocatalysis today as an effective and promising choice in green management strategies. Robust oxidation capacity, good photocatalytic activity, and high free-exciton binding energy enable the persistence of excitonic emission processes at or above room temperature. Photocorrosion and the large band gap energy are ZnO's main disadvantages. Due to its broadband energy, ZnO's light absorption is restricted in the visible light spectrum. Low photocatalytic efficiency is the consequence, as photogenerated charges quickly recombine. Several recent review publications have discussed the development and application of various ZnO nanostructures with different morphologies in light of these advantages [19, 20]. The optical, electronic, and structural characteristics of ZnO nanostructures that are changed throughout the ZnO doping process will be briefly discussed in the next section.

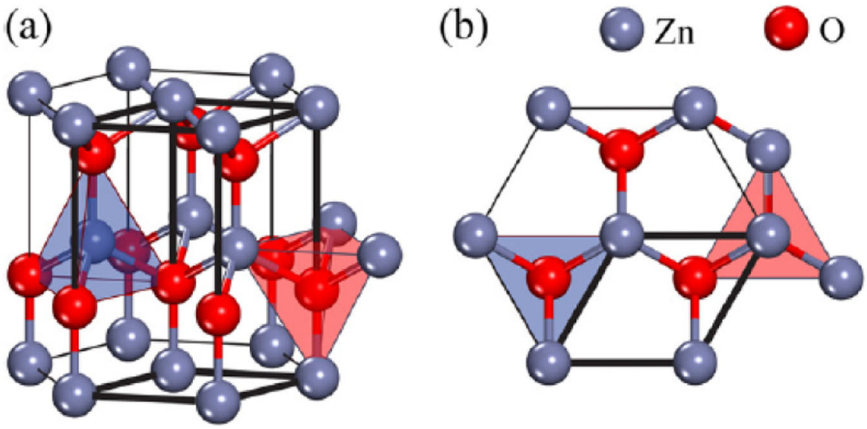

Fig. 1 Illustration depicting the crystal structures of ZnO wurtzite: (**a**) lateral view and (**b**) upper view [27]

2.1 Optical properties

At ambient temperature, ZnO exhibits a direct band-gap of 3.37 eV, a substantial exciton binding energy of 60 meV, outstanding electro-optical characteristics, and significant electrochemical reliability [21]. ZnO can be used in nanoscale applications to change or enhance its optical, electrical, and magnetic properties. Because ZnO is compatible with living things, it may be used in everyday applications without endangering human health or the environment making it an environmentally friendly material. The complete mineralization and degradation of environmental contaminants have drawn much attention to ZnO [22]. ZnO is expected to have a photocatalytic performance comparable to TiO_2, as both have almost the same band gap energy (3.2 eV). Furthermore, ZnO is comparatively less expensive than TiO2, while TiO_2 is not cost-effective for use in large-scale water treatment operations. The absorption mechanism is directly affected by the larger direct band gap, greater breakdown voltages, stronger breakdown field, and increased electron mobility of the n-type ZnO semiconductor. The main benefit of zinc oxide is by far its ability to absorb a wide range of the solar spectrum and more light quanta than some semiconducting metal oxides [23].

Using photoluminescence (PL), the luminescence characteristics of ZnO can be described. In their PL spectra, ZnO nanostructures frequently exhibit two regions: the broad visible emission zone and the UV-emission region. Photocorrosion and the large band gap energy are ZnO's main disadvantages. Due to its broadband energy, ZnO's light absorption is restricted in the visible light spectrum. Low photocatalytic efficiency is the consequence, as photogenerated charges quickly recombine [24].

2.2 Structural properties

Zinc oxide (ZnO) exhibits distinct crystal formations, typically found in the forms of rocksalt, wurtzite, or cubic (zinc blende). ZnO in a rocksalt structure is quite uncommon because it can form at severe pressure. Of the three forms, the ZnO wurtzite structure has the maximum thermodynamic stability. It is ZnO's most prevalent structure [25]. With two lattice parameters, a and c, of 0.3296 nm and 0.52065 nm, respectively, ZnO exhibits a hexagonal wurtzite crystal structure at ambient temperature and pressure. Ionicity is present in Fig. 1a, b, which represents the boundary between ionic and covalent semiconductors. The Hermann–Mauguin notation's P63mc class or the Schoenflies notation's C_{6v}^4 class are the respective classes to which the hexagonal wurtzite crystal structure belongs. In the ZnO primitive unit cell (shown as a thicker line in Fig. 1a), four oxygen ions form a tetrahedral coordination around each zinc ion, and the opposite is also true. Wurtzite ZnO exhibits a quartet of common crystal faces: the non-polar (11_20) (a-axis) and (10_10) faces, which both have a similar amount of Zn and O atoms; and the polar Zn-terminated (0001) and O-terminated (000_1) faces (c-axis orientated). It is discovered that while the polar and (1010) surfaces are stable, the (11_20) face is not as stable [26]. The X-ray diffraction (XRD) method is commonly used to estimate the lattice parameters at room temperature in an ideal wurtzite structure are $a = 3.25$ and $c = 5.20$ Å, in the ratio $c/a = 1.6$. Normally, the a-parameter falls between 3.2475 and 3.2501 Å, while the c-parameter normally runs between 5.2042 and 5.2075 Å. The concentration of foreign atoms, flaws, outer pressures, and temperature all affect how the lattice characteristics vary [27, 28].

2.3 Electronic properties

Experimental evaluations of several hypotheses have been employed to calculate and ascertain the band structure and electronic states of wurtzite ZnO [29]. One of the aspects of ZnO that has been investigated the most is its electronic properties. Generally speaking, ZnO's electrical behavior is represented by the density of states (DOS) and energy band

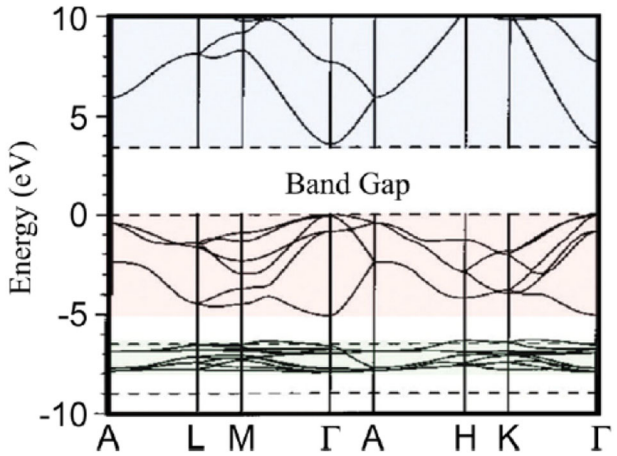

Fig. 2 Wurtzite ZnO band structures derived from density-functional theory computations [27]

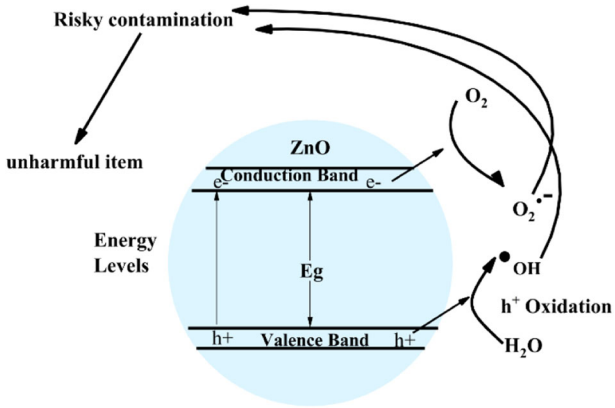

Fig. 3 A representation shows how charge carriers (e− and h+) develop on a ZnO nanostructured surface and how pollutants are degraded by photocatalysis

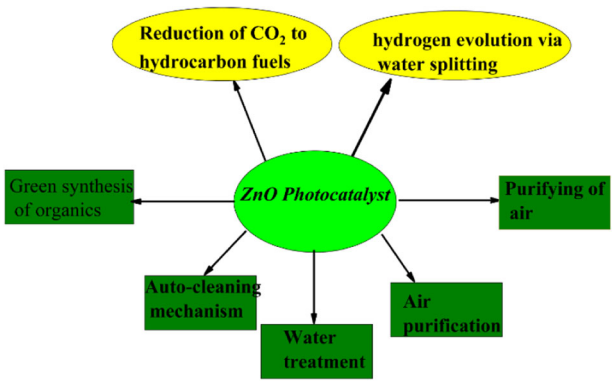

Fig. 4 ZnO nanostructures' photocatalytic uses in the fields of energy and the environment

structure, which are essential for designing devices. ZnO's typical estimated energy band structure showed a direct-type band gap in the center of the Γ k-point grid or at the Brillouin zone path G-G [30, 31]. Using the Local Density Approximation (LDA) and atomic self-interaction corrected pseudo potential (SIC-PP), the band structure computation is displayed in Fig. 2 [27]. The Zn 3d levels are linked to the bands in the valence band that are between −10 and −5 eV, while the O 2p orbitals are mostly represented by the upper 6 bands that stretch from −5 eV to 0 eV. The conduction band's (CB) initial two bands correspond to empty Zn 4s levels. This calculation indicated that the band gap value was 3.77 eV [32].

ZnO is an intrinsically n-type semiconductor because of the stoichiometry deviation and the presence of intrinsic defects such as oxygen vacancies (VO), zinc interstitials (Zni), and zinc vacancies (VZn). The existence of inherent defects such as oxygen vacancies (VO), zinc interstitials (Zni), and zinc vacancies (VZn), as well as the stoichiometry deviation, make ZnO an innately n-type semiconductor [33].

3 Principles of ZnO photocatalyst

In the petrochemicals, refinery, processing of food, and environmental remediation industries, catalysis is crucial. These chemical reactions can be accelerated by applying UV-visible irradiation to a particular semiconductor photocatalyst in certain situations. [34]. Figure 3 illustrates the general mechanism of heterogeneous photocatalysis processes.

ZnO is used as a photocatalysis material in various environmental utilization, such as the production of renewable energy through water-splitting and reduction of carbon dioxide to hydrocarbon-based fuels, green organic synthesis, automatic cleaning operations, sterilization reactions, and water and air treatment [35]. Figure 4 shows a variety of uses for ZnO photocatalysts in the energy and environmental domains.

Photocatalytic processes in ZnO are initiated by the absorption of light radiation with energy (hv) equal to or more than the ZnO band gap energy (hv ≥ Eg). The generation of holes (h^+) in the valence band (hVB+) occurs as a result of photon absorption-induced excitation and electron transfer (e^-) from the valence band (VB) to the conduction band (eCB^-) [36]. The second stage involves the migration and separation of charge carriers (e^- and h^+) to the ZnO surface. When heat or photons are released, recombination of electrons and holes may occur, which lowers the quantum efficiency of the photocatalytic process. There is a substantial association between the nature of ZnO nanostructures and many characteristics that affect the recombination rate [37]. Superoxide anion radicals (O_2^-•) and hydroxyl radicals (•OH) are produced via reduction and oxidation processes, respectively, by the extremely reactive electrons and holes on the surface of the ZnO photocatalyst.

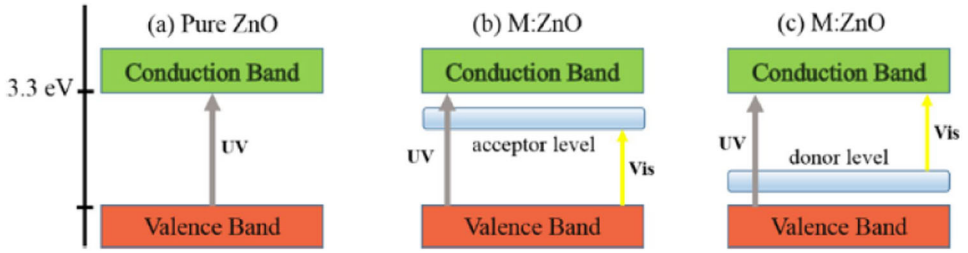

Fig. 5 Infographic illustrating the doping effect on zinc oxide's band gap energy levels: a) pristine ZnO, b) ZnO with metal-doping (donor level), and c) ZnO with metal doping (acceptor level) [42]

Since the redox potential of $O_2/O_2^{-}\bullet$ (−0.33 V vs. NHE) is less negative than the bottom level of the conduction band potential (−0.5 V vs. NHE) in ZnO, electrons can generate superoxide anion radicals. On the other hand, holes can oxidize water molecules to create hydroxyl radicals because the top of the valence band potential (+2.7 V vs. NHE) is more positive than the redox potential of $\bullet OH/H_2O$ (+2.53 V vs. NHE). These reactive radical species participate in the photocatalytic process via a set of the following reactions [38].

$$ZnO + h\upsilon \Rightarrow ZnO(h_{ob}{}^{+}e_{cb}^{-}) \quad (1)$$

$$H_2O + h_{vb}^{+} \Rightarrow \bullet OH + H^{+} \quad (2)$$

$$O_2 + e_{cb}^{-} \Rightarrow O_2^{-\bullet} \quad (3)$$

$$O_2^{-\bullet} + H^{+} \Rightarrow HO_2^{-} \quad (4)$$

$$HO_2^{-} + H^{+} \Rightarrow H_2O_2 \quad (5)$$

$$H_2O_2 + h\upsilon \Rightarrow 2\cdot OH \quad (6)$$

Risky compounds in interaction with

$$\cdot OH \text{ or } O_2^{-}. \rightleftarrows Intermediates \rightleftarrows Harmful\ Products$$

According to kinetic studies, photocatalysis's breakdown of organic pollutants follows a Langmuir–Hinshelwood principle and a quasi-first-order reaction [39]. The rate of photocatalytic decomposition (r) is denoted by

$$r = -dc(t)/d(t) = kobs\, C(t) \quad (7)$$

where the measured rate constant, kobs, and the reactant concentration, C (t), are given at time t. At extremely low concentrations, the streamlined Langmuir–Hinshelwood model yields the following apparent rate constant, or Kapp:

$$Ln\, C_o/C = kappt \quad (8)$$

Where C0 is the substance's starting concentration before photocatalysis. Hence, the photocatalytic decomposition rate is shown by the linear fit between ln(C0/C) and irradiation duration. An examined sample's photocatalytic activity is better when its Kapp value is higher.

4 Benchmarking of the doping impact of ZnO-Visible light photocatalyst

ZnO's band gap needs to be narrowed for photocatalytic processes to occur in visible light. ZnO doping can decrease the band gap in many ways, including raising the valence band maximum, reducing the conduction band minimum, and adding localized energy levels to the band gap [40]. The three distinct scenarios for producing visible-light-driven photocatalysts, like ZnO, via metal and doping, are shown in Fig. 5.

It has been demonstrated that metal doping, with less than 10 at% of foreign cations, can move the semiconductor photocatalyst's absorption edge into the visible range. When the metal cation states interact with the valence or conduction band of ZnO, band gap narrowing and intraband gap levels are generated. Metal ions are used as electron acceptors in the p-type doping seen in Fig. 5, which creates a level in the band gap below the initial conduction band. Furthermore, a level above the valence is produced by doping metal ions with n-type electron donors. Extended wavelength light can be absorbed by these recently developed states. The concentration, ionic radius, and electronegativity of the metal dopants determine whether they segregate to grain boundaries or occupy substitutional or interstitial locations in the ZnO lattice. Whereas metal doping produces mid-gap level states that increase the absorption of light to visible light, these new states have the potential to function as charge recombination centers, which could reduce photocatalytic activity [41].

By raising the valence band maximum in the nonmetal substitution scenario, substitution produces a new valence band state that causes the band gap to decrease. Consequently, nonmetal doping is less likely to create recombination centers than metal doping. Therefore, nonmetal doping works better to increase ZnO's photocatalytic activity when exposed to visible light. Surprisingly, doping should produce new band states with sufficient oxidation and reduction potential for superoxide and hydroxyl radicals to produce reactive •OH and $O_2^{-}\bullet$ radicals for photocatalytic destruction [13, 40–42].

4.1 Metalic doped ZnO

One well-known method for adjusting ZnO's band gap to make it a visible light-active photocatalyst is to dope the

crystal lattice with transition metals [40]. The ZnO host's shape, particle size, and crystallite size can all be altered by metallic doping. It is commonly known that the presence of metal doping limits the growth of ZnO, resulting in the formation of smaller nanostructures with greater surface area [43]. When metallic cations are substituted, the Zn environment in the ZnO lattice is altered, along with the electrical band structure and the introduction of many structural defects such as oxygen vacancies. Oxygen vacancies could function as effective traps for electrons and improve the efficiency of photo-generated electron/hole dissociation [44, 45].

Transition-metal dopants are often used because of their non-full d or f orbitals. The ZnO optical absorption edge extends into the visible light spectrum during doping. Doping ZnO does not modify its energy band gap value; instead, the dopants' inclusion creates mid-state gap energy that is activated by visible light [46]. This is widely acknowledged to be associated with the sp-d spin exchange interaction between localized d-electrons of the transition metal ions (TM ion) and ZnO band-edge electrons. Three types of transitions can be identified based on the electrical transitions linked to TM-doped ZnO nanostructures. These transitions are explained as follows: i) charge transfer transitions between the host CB and the dopant d-state, as well as between the host VB and the dopant d-state; ii) dopant-induced d-d inner transition; and iii) stimulation of electrons from the VB to CB of the ZnO host. Transitions of types (ii) and (iii) can happen in visible light. After persisting in ZnO's VB, photogenerated holes travel to the surface where they form active •OH radicals. O_2^-• is created when the excited electrons react with the adsorbed O2 while they are trapped in the TM dopant sites. These specimens take part in processes of photocatalytic degradation [47].

ZnO photocatalyst activity can be enhanced by the oxidation states of certain transition metals, such as Fe and Cu. When ZnO is doped with the right amounts of Fe and Cr, ferromagnetic photocatalysts are formed. This is useful for gathering photocatalysts after the degradation reaction from the surrounding environment. Additionally, several investigations have demonstrated a considerable decrease in ZnO photocatalytic activity following doping with TM ions such as Fe, Co, Ni, and Mn. The function of non-metal dopants will be studied in the ensuing sections.

4.2 Non-metalic doped ZnO

ZnO nonmetal doping has been studied extensively as a potential oxygen atom replacement. Various photocatalysts have been produced that show promise when exposed to visible light. As was previously mentioned, the band gap reduces as a result of the hybridization of ZnO's O 2p states and nonmetal dopant orbitals raising the valence band's upper edge. Effective nonmetal dopants must have two primary characteristics: they must be smaller than lattice O atoms and have an electronegativity lower than that of oxygen [48]. When nonmetals like carbon (C), nitrogen (N), and sulfur (S) are doped into ZnO, the valence band is broadened and intermediate energy levels are formed. This results in visible-light photocatalytic activity. Nitrogen is the nonmetal dopant that has garnered the greatest attention up to this point. This is because of its benefits, which include low production energy, excellent solubility in the N 2p and O 2p energy states, and similarity between nitrogen and oxygen ionic radii. Band gap shrinking results from the hybridization of N 2p and O 2p states, which raises the valence band's upper edge [49, 50].

Different characteristics of N-substituted ZnO can be seen according to methods of preparation and source of nitrogen doping. Ferrari-Lima et al. reported that N-doped ZnO derived from ammonium hydroxide has a higher specific surface area. [51]. They explained this by saying that the presence of nitrogen causes controlled crystallite nucleation and growth. In contrast, Wu [52] found that when N-doped ZnO was calcined with NH4NO3 as the nitrogen source, the specific surface area of the ZnO sample decreased as a result of a breakdown of tiny pores.

The second most common method of nonmetal doping ZnO is carbon doping, which has attracted a lot of attention lately. Through DFT simulations, Pan et al. [53] investigated the structural and magnetic characteristics of both pure and C-doped ZnO. Carbon inclusion is observed with carbon oxidation numbers ranging from −4, where an oxygen atom (CO) is replaced, to +4, where carbonate species (CZn + 2Oi) are created after the formation energies of carbon doping were calculated. There is also evidence of carbon doping on Zn sites (CZn) and interfacial carbon (Ci). By ab initio methods to compute the formation energy of C doping, Tan et al. [54] showed that the formation energy of CZn and CZn + 2Oi increased with decreasing partial pressure of oxygen and that the oxygen-rich environment was conducive to the development of CO/CO_2 species. Additionally, they discovered that the acceptor state, CZn + 2Oi, had a relatively large production energy, and the donor state, CZn, had a comparatively low production energy.

It is proposed that sulfur doping of ZnO can alter its optical, electrical, and photocatalytic properties because S has a higher Bohr radius than O due to the difference in their electronegativity. S-doped ZnO's photocatalytic qualities in visible light have not been well studied and are subject to considerable debate. In particular, there have been reports on the Burstein-Moss effect-caused band gap broadening resulting from S doping [55]. However, other investigations have reported a decrease in the band gap. It is

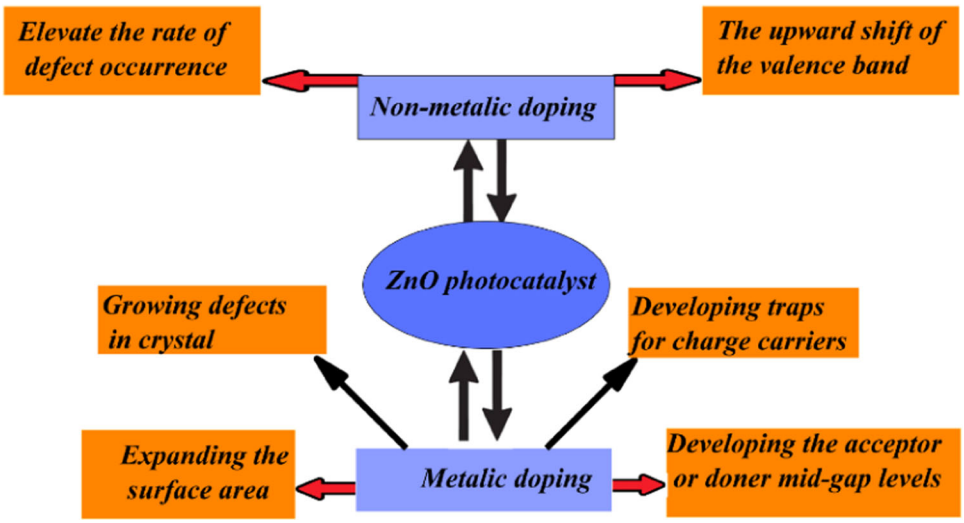

Fig. 6 Characteristics of metal and nonmetal doping to improve ZnO photocatalyst activity in visible light

necessary to clarify these conflicting findings on S-doped ZnO from both theoretical and experimental perspectives by employing particular concentration and doping techniques. Research on S-doped ZnO, both theoretical and experimental, can shed light on the function of S atom doping as well as the characteristics of the material. DFT calculations were used by Zhang et al. to investigate the connection between sulfur doping and photocatalytic activity [56]. They claimed that the physical properties of S-doped ZnO are influenced by the different S substitutional sites in the ZnO lattice. In SO-doped ZnO, the O 2p states combine with the S 3p levels, which are located above the valence band, to shrink the band gap. The slowing of electron/hole recombination and the entry of VO and VZn into the ZnO crystal lattice are the main factors impacting the photocatalytic activity of S-doped ZnO, and they were discussed.

For visible light-responsive photocatalysts, the doping strategy, as shown in Fig. 6, is a helpful way to alter the photocatalytic activity of ZnO nanostructures. The doping process's general characteristics include altering the products' morphology and generating different defects including oxygen vacancies, dislocation, and crystal deformation. When the right kind and dopant concentration are added, these flaws can significantly increase ZnO's photocatalytic activity.

5 ZnO's progress in eliminating water pollutants

The most hazardous organic substances are phenolic compounds, dyes, and persistent organic pollutants. Because of their extreme danger to human well-being, marine organisms, and the natural world, these compounds have long been the subject of concern. Because organic contaminants can accumulate in the waters as they gradually make their way up the food chain, they must be removed from industrial effluent. To get rid of the organic contaminants, several techniques have been devised and implemented [56–59]. However, the majority of these techniques are inappropriate for field applications because they call for labor-intensive, time-consuming procedures, extremely precise sample preparation, expensive or specialized instruments, poor removal efficiency, and lengthy turnaround times. Modern photodegradation technique has been widely used because of its capacity to eliminate persistent organic pollutants, dyes, and phenolic chemicals from wastewater. This technology is gradually finding its way into a wide range of businesses and is even starting to be sold internationally. Because of its low cost and photosensitivity, ZnO has been a popular option for use as a photocatalyst to remove specific contaminants. ZnO photocatalyst-mediated photodegradation of organic contaminants is a straightforward, adaptable, and economical remediation method [60–63]. Numerous studies have demonstrated that using ZnO as a photocatalyst under UV or visible light reduces the concentration of pollutants in water. Table 2 displays the effective use of ZnO in photodegradation to eliminate dyes and water contaminants.

6 Electron hole recombination in ZnO

The high rate of electron/hole recombination greatly reduces the photocatalytic activity of individual photocatalysts. Researchers are focusing more on the idea of enhancing photocatalytic activity by preventing their recombination. Several strategies for modification have been developed to address the aforementioned issues. Including plasma excitonic components and upconversion influences into materials for photocatalysis significantly broadens the ability to absorb and use light, which has important implications for developing novel effective

Table 2 ZnO-mediated photocatalytic degradation of certain organic pollutants

Contaminant	Conditions of the experiment	Rate of degradation	Ref
MB	20 mg in 50 mL catalyst. And 10 mg L^{-1} contaminant. 300 W Xe lamp as a Light source	Efficiency of Photodegradation: ~97%	[91]
MB	0.02 g in 100 mL catalyst, and 20 mg L^{-1} contaminant. 40 W UV-C and 40 W Xe lamps light sources	Efficiency of Photodegradation: 98%	[92]
MO and RhB	0.1 g in 100 mL catalyst, 10^{-4} mol L^{-1} contaminant, 500 W halogen lamp as the light source.	Efficiency of Photodegradation: 88% (MO) and76% (Rh B).	[93]
MO	50 mg in 50 mL catalyst, 10 mg L^{-1} reactant, 100 W high-pressure light source.	Efficiency of Photodegradation: 90% at light and vibration, 60% at vibration, and 55% with light.	[94]
Crystal violet dye	0.1 g in 100 mL catalyst, 25 µM reactant, and single Heber tungsten lamp as a light source (500 W).	Efficiency of photodegradation 98% (UV–Vis)	[95]
RhB, MO, and MB	50 mg in 100 mL catalyst, 10 mg L^{-1} reactant, and xenon lamp (75 W) visible light with UV cut off filters.	Efficiency of photodegradation 75.3% (MO), 88.08% (RhB), and 93.9% (MB).	[96]
MB	10 mg in 50 mL catalyst, 30 mg L^{-1} reactant, and 300 W xenon lamp as the light source.	Efficiency of Photodegradation: 80%	[97]
Leachate	400 cm^2 coated area of 60 g/m^2 catalyst, 800 mg L^{-1} reactant, and 32 W light source.	Efficiency of photodegradation: 61%	[98]
Fluorophenol (phenolics)	32 W Hg lamp as a light Source, ZnO 2 g/L catalyst, and 100 mg/L reactant.	Efficiency of photodegradation: 60%	[99]
Chlorophenol (4CP)	2 g/L catalyst, 50 mg/L reactant, and 6 W UV lamp as a light source.	the efficiency of photodegradation: 50%	[100]
Phenylhydrazi-ne	0.25 g catalyst, 20 mg/L reactants, and 75 W Hg lamp as a light source.	the efficiency of photodegradation: 37%	[101]
Ortho-nitrophenol	0.25 g/L photocatalyst, 10 mg/L reactant, and lamp with 30 W UV-C light source.	the efficiency of photodegradation: 98%	[102]
Acid Red 18	4 g/L catalyst, 0.0005 M reactant, and medium pressure 64 W lamp as a light source.	the efficiency of photodegradation: 100%	[103]
Methyl Orange	1 g/L^{-1} catalyst, L/L reactant, and high pressure 125 W Hg Lamp as a light source.	Efficiency of photodegradation: 60%	[104]
Orang II (OII)	0.5 g L^{-1}, and 18 W UV lamp as a light source.	Efficiency of photodegradation: 100%	[105]
Acridine orange	5 g/L catalyst, 0.00005 M reactant, and 500 W halogen lamp as a light source.	Efficiency of Photodegradation: 98%	[106]
Methyl Green (MG)	0.25 g/L catalyst, 50 mg/L reactant, and 30 W visible light lamp source.	Efficiency of Photodegradation: 100%	[107]
Methylene Blue (MB)	20 mM catalyst, and 500 W tungsten-halogen light source.	Efficiency of Photodegradation: 80%	[74]
Phenol	292.2 mg L^{-1} reactant, 1 g L^{-1} catalyst, and 1500 xenon lamp light source.	Efficiency of Photodegradation: 42%	[108]
Rhodamine	0.10 g of catalyst, 100 mL of 5 ppm RhB, and 300 W halogen lamp as light source.	Efficiency of Photodegradation: 99%	[72]

photocatalysts with wide-spectrum absorption characteristics. Metal doping and morphology adjustment can also partially prevent complications. Apart from these methods, some other methods have also been investigated and documented in dual semiconductors. These methods include the creation of heterojunctions between semiconductors and the utilization of photocatalytic effects to construct external circuits, both of which can significantly enhance photocatalytic performance.

When a photocatalyst is exposed to the right amount of energy, electron $(e^-)^-$ electron–hole (h+) pairs are generated throughout the entire catalyst. Only an electron and an electron hole on a photocatalyst surface cause it to interact with a substrate. There are more $(e^- + h^+)$ pairs on the surface of a photocatalyst if the movement of electron–hole, and electron on the surface is fewer than recombination. This boosts process efficiency [64]. Therefore, the longer the lifetime of photo-excited electron holes and electrons, the higher the photocatalyst's impact.

Photocatalysts are typically semiconductor solid oxides with the ability to absorb light and produce pairs of

electrons when it does so. These electron–hole pairs oxidize the materials that are already present at the surface to relatively safe materials through their reaction [65, 66]. When photocatalyst material such as ZnO is exposed to light with a wavelength that is equal to or greater than its band gap, an electron is moved from its valence band to the conduction band, and an electron–hole pair is created. The electron can react with other substances and electron donors on the surface, or it can join with the hole once more to release energy. However, it has been practically found that when the rate of electron–hole recombination is high, the photocatalytic activity is low [67–71]. The spectrums of photoluminescence analysis (PL), investigate the electron–hole recombination rate of various materials. Low PL spectrum intensity materials have low photogenerated charge carrier recombination rates, whereas high PL spectrum intensity materials have high recombination rates. Based on these facts, one can determine the recombination rate of the photocatalyst material and accordingly predict the photocatalytic activity. Various reports have been focused on the photocatalytic activity of the ZnO depending on the electron–hole recombination rate. In this section, we will critically demonstrate the impact of this rate on the overall performance of the ZnO photocatalyst.

Reyhaneh Saffari et al. developed pure and P-ZnO microparticles by the hydrothermal technique and employed them for the photocatalytic degradation of the RhB contaminant [72]. The optimum doped sample exhibits a reduced intensity of band emission compared to pure ZnO, indicating a decrease in electron–hole recombination in this sample. Adding P to the ZnO structure creates some midgap levels between the conduction and valence bands in the structure. Since P acts as a separating center in the structure, this can facilitate the separation of electron–hole pairs more successfully. The best electron–hole pair separation was found in the P-ZnO1.8% with the lowest peak intensity, which is likely why it has higher photocatalytic activity.

Pure and S-incorporated ZnO nanoparticles were synthesized hydrothermally by Zahra Mirzaeifard et al., and the results were used to degrade the RhB dye [73]. Examining the electron transitions and lifetime of the electron–hole pairs created by light radiation is made easy with the help of the PL spectrum. Their PL investigation has shown that All pure and S-ZnO nanoparticles, have PL spectra with three broad peaks: one sharper peak at about 405 nm, another broad peak at about 430 nm, and a wide peak at about 385 nm. Near band-edge UV emission is represented by the peak at about 385 nm. The presence of a single oxygen vacancy in the ZnO lattice, caused by radiative electron–hole recombination at the oxygen vacancy sites, is the cause of the other two PL peaks [73].

Supamas Danwittayakula et al. produced zinc oxide/zinc tin oxide (ZnO/ZTO) nanocomposites on porosity ceramic bases by employing an easy and affordable hydrothermal process for the photocatalytic degradation of organic dyes [74]. They combined ZnO and ZTO to increase photocatalytic activity even further and discovered that ZnO/15ZTO was a more effective photocatalyst, resulting in a 16% improvement in degradation efficiency. This improvement was ascribed to the composites' ability to reduce electron–hole recombination through charge carrier separation. Furthermore, when exposed to solar radiation, ZnO/15ZTO demonstrated 50% photocatalytic degradation efficiency and 77% COD elimination of textile wastewater. A highly promising photocatalyst for solar photocatalytic applications is the ZnO/ZTO monolith.

To improve the organic matter removal effectiveness in water, Jungsu Choi et al. synthesized 3D structured Pd/ZNO on the developed electrospun nanofibers and investigated ways to reduce electron–hole recombination via the photocatalytic process and maximize the surface area [75]. To carry out water treatment, ZnO was grown on Pd-coated nanofiber. This enhanced surface area and suppression of electron–hole recombination boost OM removal efficiency. They indicated that the extra Pd layer inhibits electron–hole recombination as shown in Fig. 7.

Increased photocatalytic and photocurrent characteristics of porous ZnO thin film with Ag nanoparticles were reported by Lv et al. [75]. The information regarding the recombination of photogenerated electrons and holes is provided by photoluminescence (PL). Before diffusing to the ZnO surface, the excited electrons recombine with the holes, and this irradiative release of energy produces fluorescence. They showed that the recombination of photogenerated electron–hole pairs close to the band boundaries may be responsible for the UV emission band. Additionally, they observed that when degrading MO solution, the Ag/ZnO thin film had higher photocurrent and photocatalytic activity than the bare ZnO. The Schottky barrier that developed between ZnO and Ag nanoparticles is thought to be the cause of this improvement, as it improved separation and reduced recombination of photogenerated electron–hole pairs at the interface.

ZnO nanoparticles with varying defect concentrations have been produced by Bhatia et al. using a straightforward combustion process at 7000 °C and air quenching as a final step [76]. They applied the advantage of the PL spectra of both air-quenched and pure ZnO, which exhibit a broad emission peak at 450 nm that is linked to defect levels, or oxygen vacancies. During photocatalytic reactions, these oxygen vacancies may function as electron acceptors, lowering the rate of electron–hole recombination. The recombination of photogenerated charge carriers was inhibited by the increase in surface oxygen vacancy, leading to an enhancement in photocatalytic activity.

ZnO nanoparticles (NPs) and strontium-doped ZnO nanoparticles developed by the co-precipitation method

were reported by Raj et al. [77]. They discovered that inherent flaws caused a sequence of visible emissions between 400 and 560 nm, and the photoluminescence (PL) spectrum shows that UV emission is strongly close to the band-edge area (392 nm). RhB dye kinetic tests show that the degradation rate has increased as dopant concentration has increased. As seen in the FESEM images of Fig. 8a–h, it is evident that the nanoparticles' average diameters fall within the nanometer range. The produced nanoparticles are seen to have a high connection and to be evenly dispersed throughout the surface. The enhanced photocatalytic activity is attributed to effective charge separation, enhanced visible light absorption, inhibition of electron–hole pair recombination, and improved adsorptiveness of RhB dye molecule on the surface of the pure and Sr-doped ZnO nanoparticles. Furthermore, the results show that strontium-doped ZnO NPs have better photocatalytic activity as seen by the decrease in total organic carbon.

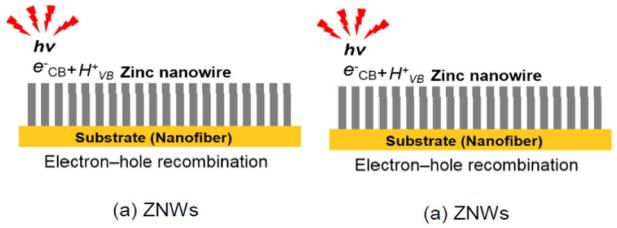

Fig. 7 The Pd-coating on the nanofiber that inhibits electron–hole recombination [75]

7 Conclusion

Since the photocatalytic procedure relies on the creation of electron or hole pairs through band gap radiation, combining various semiconductor oxides appears to help achieve potentially higher photocatalytic activity and, in turn, more efficient electron/hole pair separation under irradiation. In conclusion, this review summarized recent ZnO photocatalysis application developments in water treatment. Following an introduction to the photocatalytic process' mechanism and ZnO's characteristics, a detailed demonstration of the most current developments in ZnO photocatalytic removal of many typical water pollution categories was given, along with a few new photocatalysts. Through the synergistic effect of composite components, photocatalytic performance-enhancing solutions were identified. Although there have been some notable developments recently, the effectiveness of degradation and recycling occupancy remains poor and impractical. This review shows that the effectiveness of photocatalytic reactions is greatly influenced by every stage of the process, involving charge separation, recombination, transport, adsorption, excitation, and semiconductor surface response. ZnO hybrid photocatalyst with improved interfacial charge transfer to adsorbed pollutants, longer charge carrier lifetimes, and more efficient charge separation were the outcomes of coupled semiconductors formed by ZnO and other metal oxides, such as TiO_2, SnO_2, Fe_2O_3, WO_3, and so forth. In addition, incorporating hybrid materials significantly enhances the ZnO photocatalyst's optical and physical characteristics. To attain optimal efficiency, other factors that must be considered include the rate of degradation,

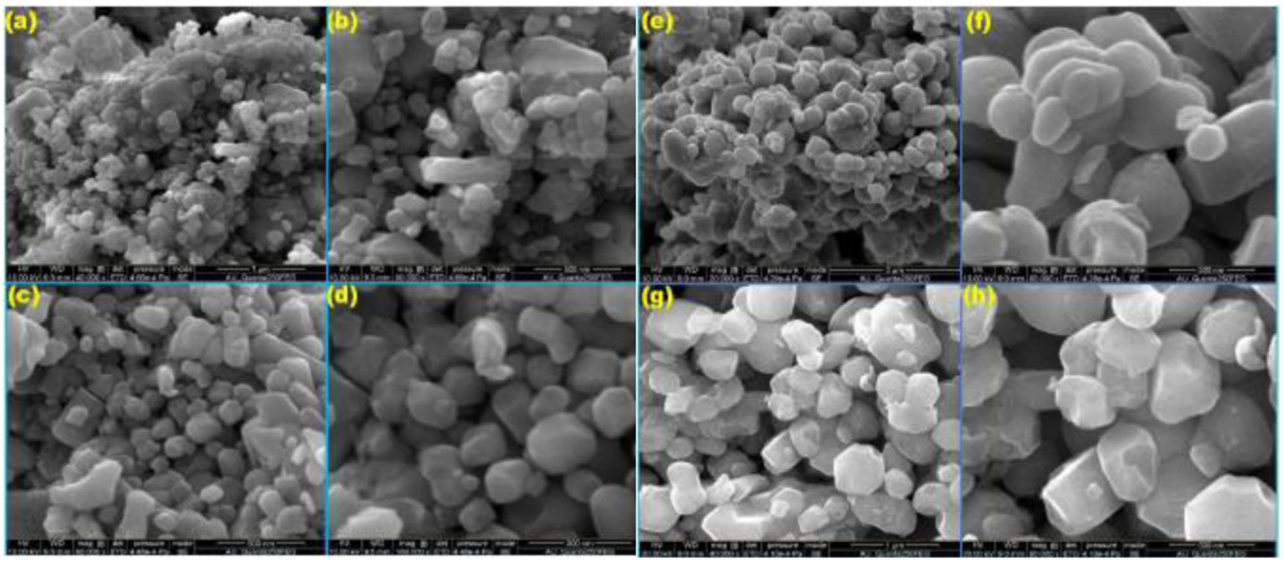

Fig. 8 SEM Images of pure and Sr-doped ZnO NPs: (**a**, **b**) ZnO NPs (**c**, **d**) 2% Sr-doped ZnO NPs (**e**, **f**) 4% Sr-doped ZnO NPs (**g**, **h**) 6% Sr-doped ZnO NPs [75]

temperature, pH, charged type of contaminants, reactor, and source of light. Thus, when developing and producing multipurpose semiconductor photocatalysts for the photocatalytic treatment of organic contaminants, all parameters had to be taken into account and meticulously tuned.

7.1 Future challenges and prospects

Due to its high photocatalytic activity, photostability, and nontoxicity, modified ZnO photocatalyst is expected to find industrial use in the future. To improve its photocatalytic activity under direct sunlight irradiation, however, more modifications are required to minimize recombination losses and reduce the band gap energy. Therefore, the modeling study is necessary to develop an effective photoreactor or system for organic dye, phenolic chemicals, and long-lasting organic pollutants in our wastewater stream and to gain greater insight into the photocatalytic oxidation degradation mechanism.

8 Availability of data and materials

The data are available in the manuscript.

Acknowledgements The authors thank the Department of Physics, University of Babylon, Iraq, for their support.

Author contributions Alaa Nihad wrote the manuscript, and the other remaining authors have contributed in results analysis. For this paper, all authors reviewed all manuscripts from valuable scientific literature as they summarized the findings of existing literature. So, readers can get an idea about the existing knowledge on the topic without having to read all the published research in the field.

Compliance with ethical standards

Conflict of interest The authors declare no competing interests.

References

1. Chellam S, Clifford DA (2002) Physical–chemical treatment of groundwater contaminated by leachate from surface disposal of uranium tailings. J Environ Eng 128(10):942–952
2. Wang H, Liu R, Qu J, Fan M, Li H (2009) Pilot-scale treatment of waste-water from carbon production by a combined physical–chemical process. J Chem Technol Biotechnol Int Res Process Environ Clean Technol 84(7):966–971
3. Radjenović J, Petrović M, Ventura F, Barceló D (2008) Rejection of pharmaceuticals in nanofiltration and reverse osmosis membrane drinking water treatment. Water Res 42(14):3601–3610
4. Sharma K, Hasija V, Malhotra M, Verma PK, Khan AAP, Thakur S, Raizada P (2024) A review of CdS-based S-scheme for photocatalytic water splitting: synthetic strategy and identification techniques. Int J Hydrogen Energy 52:804–818
5. Kang GD, Cao YM (2012) Development of antifouling reverse osmosis membranes for water treatment: a review. Water Res 46(3):584–600
6. Khan AAP, Sudhaik A, Raizada P, Khan A, Rub MA, Azum N, Asiri AM (2023) AgI coupled SiO_2@ CuFe2O4 novel photocatalytic nano-material for photo-degradation of organic dyes. Catal Commun 179:106685
7. Ayyildiz O, Peters RW (2004) Synergy of combined sonication and vapor stripping treatment in the removal of PCE from water. Fresenius Environ Bull 13(12):1515–1517
8. Malhotra M, Sudhaik A, Raizada P, Ahamad T, Nguyen VH, Van Le Q, Singh P (2023) An overview on cellulose-supported photocatalytic materials for the efficient removal of toxic dyes. Ind Crops Prod 202:117000.
9. Li Y, Xie W, Hu X, Shen G, Zhou X, Xiang Y, Fang P (2010) Comparison of dye photodegradation and its coupling with light-to-electricity conversion over TiO2 and ZnO. Langmuir 26(1):591–597
10. Mondal C, Pal J, Ganguly M, Sinha AK, Jana J, Pal T (2014) A one pot synthesis of Au–ZnO nanocomposites for plasmon-enhanced sunlight driven photocatalytic activity. N J Chem 38(7):2999–3005
11. Tian C, Zhang Q, Wu A, Jiang M, Liang Z, Jiang B, Fu H (2012) Cost-effective large-scale synthesis of ZnO photocatalyst with excellent performance for dye photodegradation. Chem Commun 48(23):2858–2860
12. Kumar SG, Rao KK (2015) Zinc oxide based photocatalysis: tailoring surface-bulk structure and related interfacial charge carrier dynamics for better environmental applications. RSC Adv 5(5):3306–3351
13. Li J, Wu N (2015) Semiconductor-based photocatalysts and photoelectrochemical cells for solar fuel generation: a review. Catal Sci Technol 5(3):1360–1384
14. Hunge YM, Yadav AA, Kang SW, Mohite BM (2023) Role of nanotechnology in photocatalysis application. Recent Pat Nanotechnol 17(1):5–7
15. Dhull P, Sudhaik A, Raizada P, Thakur S, Nguyen VH (2023) Van Le Q, Kumar N, Khan AAP, Marwani HM, Selvasembian R, Singh, P (2023) An overview on ZnO-based sonophotocatalytic mitigation of aqueous phase pollutants. Chemosphere 333:138873
16. Hunge YM, Yadav AA, Kang SW, Lim SJ, Kim H (2023) Visible light activated MoS2/ZnO composites for photocatalytic degradation of ciprofloxacin antibiotic and hydrogen production. J Photochem Photobiol A Chem 434:114250
17. Sharma K, Kumar A, Ahamad T, Van Le Q, Raizada P, Singh A, Singh P (2023) Sulphur vacancy defects engineered metal sulfides for amended photo (electro) catalytic water splitting: a review. J Mater Sci Technol 152:50–64
18. Ali RS, Sharba KS, Jabbar AM, Chiad SS, Abass KH, Habubi NF (2020) Characterization of ZnO thin film/p-Si fabricated by vacuum evaporation method for solar cell applications. Neuro-Quantology 18(1):26
19. Hunge YM, Yadav AA, Kang SW, Kim H (2022) Facile synthesis of multitasking composite of Silver nanoparticle with Zinc oxide for 4-nitrophenol reduction, photocatalytic hydrogen production, and 4-chlorophenol degradation. J Alloy Compd 928:167133
20. Kale V, Hunge YM, Kamble SA, Deshmukh M, Bhoraskar V S, Mathe VL (2021) Modification of energy level diagram of nanocrystalline ZnO by its composites with ZnWO4 suitable for sunlight assisted photo catalytic activity. Mater Today Commun 26:102101
21. Hunge YM, Yadav AA, Mathe VL (2019) Photocatalytic hydrogen production using TiO_2 nanogranules prepared by hydrothermal route. Chem Phys Lett 731:136582
22. Bharti J, Kumar JS, Kumar SS, V, Kumar A, Kumar D (2022) A review on the capability of zinc oxide and iron oxides nanomaterials, as a water decontaminating agent: adsorption and photocatalysis. Appl Water Sci 12(3):46

23. Mahadik MA, Shinde SS, Hunge YM, Mohite VS, Kumbhar SS, Moholkar AV, Bhosale CH (2014) UV assisted photoelectrocatalytic oxidation of phthalic acid using spray deposited Al doped zinc oxide thin films. J Alloy Compd 611:446–451
24. Gomez-Solís C, Ballesteros JC, Torres-Martínez LM, Juárez-Ramírez I, Torres LD, Zarazua-Morin ME, Lee SW (2015) Rapid synthesis of ZnO nano-corncobs from Nital solution and its application in the photodegradation of methyl orange. J Photochem Photobiol A Chem 298:49–54
25. Yadav AA, Hunge YM, Kang SW (2021) Porous nanoplate-like tungsten trioxide/reduced graphene oxide catalyst for sonocatalytic degradation and photocatalytic hydrogen production. Surf Interfaces 24:101075
26. Yadav AA, Hunge YM, Kang SW, Fujishima A, Terashima C (2023) Enhanced photocatalytic degradation activity using the V2O5/RGO composite. Nanomaterials 13(2):338
27. Pasquarelli RM, Ginley DS, O'Hayre R (2011) Solution processing of transparent conductors: from flask to film. Chem Soc Rev 40(11):5406–5441
28. Jagadish C, & Pearton SJ (eds) (2011) Zinc oxide bulk, thin films and nanostructures: processing, properties, and applications. Elsevier
29. Hunge YM, Yadav AA, Kang SW (2022) Photocatalytic degradation of eriochrome black-T using BaWO4/MoS2 Composite. Catalysts 12(10):1290
30. Ma X, Wu Y, Lv Y, Zhu Y (2013) Correlation effects on lattice relaxation and electronic structure of ZnO within the GGA+ U formalism. The. J Phys Chem C 117(49):26029–26039
31. Tuama AN, Abbas KH, Hamzah MQ, Mezan SO, Jabbar AH, Agam MA (2020) An overview on characterization of silver/cuprous oxide nanometallic (Ag/Cu2O) as visible light photocatalytic. Int J Adv Sci Technol 29(3):5008–5018
32. Abass KH, Mohammed MK (2019) Fabrication of ZnO: Al/Si solar cell and enhancement its efficiency via Al-doping. Nano Biomed Eng 11(2):170–177
33. Ma Z, Ren F, Ming X, Long Y, Volinsky AA (2019) Cu-doped ZnO electronic structure and optical properties studied by first-principles calculations and experiments. Materials 12(1):196
34. Hunge YM, Yadav AA, Mahadik MA, Bulakhe RN, Shim JJ, Mathe VL, Bhosale CH (2018) Degradation of organic dyes using spray deposited nanocrystalline stratified WO3/TiO2 photoelectrodes under sunlight illumination. Optical Mater 76:260–270
35. Abebe B, Murthy HA, Amare E (2020) Enhancing the photocatalytic efficiency of ZnO: Defects, heterojunction, and optimization. Environ Nanotechnol Monit Manag 14:100336
36. Mutalib AA, Jaafar NF (2022) ZnO photocatalysts applications in abating the organic pollutant contamination: a mini review. Total Environ ResThemes 3-4:100013
37. Abdul Hamid SB, Teh SJ, Lai CW (2017) Photocatalytic water oxidation on ZnO: a review. Catalysts 7(3):93
38. Lam SM, Sin JC, Abdullah AZ, Mohamed AR (2012) Degradation of wastewaters containing organic dyes photocatalysed by zinc oxide: a review. Desalin Water Treat 41(1-3):131–169
39. Liu B, Zhao X, Terashima C, Fujishima A, Nakata K (2014) Thermodynamic and kinetic analysis of heterogeneous photocatalysis for semiconductor systems. Phys Chem Chem Phys 16(19):8751–8760
40. Coronado JM, Fresno F, Hernández-Alonso MD, Portela R (eds) (2013) Design of advanced photocatalytic materials for energy and environmental applications. vol 71 Springer, London
41. Chen X, Shen S, Guo L, Mao SS (2010) Semiconductor-based photocatalytic hydrogen generation. Chem Rev 110(11):6503–6570
42. Moosavi F, Neri G (2023) Effect of Pb doping on the structural, optical and electrical properties of sol–gel ZnO nanoparticles. Discov Mater 3(1):30
43. Wu C, Shen L, Zhang YC, Huang Q (2011) Solvothermal synthesis of Cr-doped ZnO nanowires with visible light-driven photocatalytic activity. Mater Lett 65(12):1794–1796
44. Barick KC, Singh S, Aslam M, Bahadur D (2010) Porosity and photocatalytic studies of transition metal doped ZnO nanoclusters. Microporous Mesoporous Mater 134(1-3):195–202
45. Thennarasu G, Sivasamy A (2013) Metal ion doped semiconductor metal oxide nanosphere particles prepared by soft chemical method and its visible light photocatalytic activity in degradation of phenol. Powder Technol 250:1–12
46. Sharma DK, Shukla S, Sharma KK, Kumar V (2022). A review on ZnO: Fundamental properties and applications. Materials Today: Proceedings 49:3028–3035
47. Yang Y, Li Y, Zhu L, He H, Hu L, Huang J, Ye Z (2013) Shape control of colloidal Mn doped ZnO nanocrystals and their visible light photocatalytic properties. Nanoscale 5(21):10461–10471
48. Sanakousar FM, Vidyasagar CC, Jiménez-Pérez VM, Prakash K (2022) Recent progress on visible-light-driven metal and non-metal doped ZnO nanostructures for photocatalytic degradation of organic pollutants. Mater Sci Semicond Process 140:106390
49. Zong X, Sun C, Yu H, Chen ZG, Xing Z, Ye D, Lu GQ(M), Li X, Wang L (2013) J Phys Chem C 117(10):4937–4942
50. Sun L, Shao Q, Zhang Y, Jiang H, Ge S, Lou S, Guo Z (2020) N self-doped ZnO derived from microwave hydrothermal synthesized zeolitic imidazolate framework-8 toward enhanced photocatalytic degradation of methylene blue. J colloid interface Sci 565:142–155
51. Ferrari-Lima AM, De Souza RP, Mendes SS, Marques RG, Gimenes ML, Fernandes-Machado NRC (2015) Photodegradation of benzene, toluene and xylenes under visible light applying N-doped mixed TiO_2 and ZnO catalysts. Catal Today 241:40–46
52. Wu C (2014) Facile one-step synthesis of N-doped ZnO micropolyhedrons for efficient photocatalytic degradation of formaldehyde under visible-light irradiation. Appl Surf Sci 319:237–243
53. Pan H, Yi JB, Shen L, Wu RQ, Yang JH, Lin JY, Yin JH (2007) Room-temperature ferromagnetism in carbon-doped ZnO. Phys Rev Lett 99(12):127201
54. Tan ST, Sun XW, Yu ZG, Wu P, Lo GQ, Kwong DL (2007) p-type conduction in unintentional carbon-doped ZnO thin films. Appl Phys Lett 91(7):072101.
55. Shen G, Cho JH, Yoo JK, Yi GC, Lee CJ (2005) Synthesis and optical properties of S-doped ZnO nanostructures: nanonails and nanowires. J Phys Chem B 109(12):5491–5496
56. Hamzah MQ, Agam MA, Tuama AN, Jameel MH (2023). Preparation and characterization of polystyrene nanosphere. In: AIP Conference Proceedings vol 2475 no 1 AIP Publishing
57. Mezan SO, Jabbar AH, Hamzah MQ, Tuama AN, Hasan NN, Roslan MS, Agam MA (2019) Synthesis, characterization, and properties of polystyrene/SiO2 nanocomposite via sol-gel process. In: AIP Conference Proceedings vol 2151 no 1 AIP Publishing
58. Jabbar AH (2019) Enhanced bioactivity of polystyrene-silver nanocomposite (PS/Ag NCs)-an antimicrobial study". AIP Conf Proc 2151(1):020002
59. Mario J, Goran S, Darija O, Fredi F (2011) Effects of speed, agility, quickness training method on power performance in elite soccer players. J Strength Cond Res 255:1285–1292
60. Roy N, Chakraborty S (2021) ZnO as photocatalyst: An approach to waste water treatment. Mater Today: Proc 46:6399–6403
61. Jain B, Hashmi A, Sanwaria S, Singh AK, Susan MABH, Singh A (2020) Zinc oxide nanoparticle incorporated on graphene oxide: an efficient and stable photocatalyst for water treatment through the Fenton process. Adv Compos Hybrid Mater 3:231–242

62. Zaidi Z, Siddiqui SI, Fatima B, Chaudhry SA (2019) Synthesis of ZnO nanospheres for water treatment through adsorption and photocatalytic degradation: modelling and process optimization. Mater Res Bull 120:110584
63. Baruah S, K Pal S, Dutta J (2012) Nanostructured zinc oxide for water treatment. Nanosci Nanotechnol Asia 2(2):90–102
64. Tuama AN, Al-Bermany E, Alnayli RS, Abass KH, Abdali K, Jameel MH (2024) A critical review of the evaluation of Sio_2-incorporated Tio_2 nanocomposite for photocatalytic activity. Silicon 16:2323–2340
65. Calzada LA, Castellanos R, García LA, Klimova TE (2019) TiO2, SnO2 and ZnO catalysts supported on mesoporous SBA-15 versus unsupported nanopowders in photocatalytic degradation of methylene blue. Microporous Mesoporous Mater 285:247–258
66. Jameel MH, Mayzan MZHB, Roslan MSB, Agam MAB, Jabbar AH, Badi KM, Tuama AN (2024) Bandgap engineering and tuning of electronic and optical properties of hetero-atoms-doped-graphene composites by density functional quantum computing for photocatalytic applications. Catalysis Lett 1–12
67. Seo YS, Oh SG (2019) Controlling the recombination of electron–hole pairs by changing the shape of ZnO nanorods via sol-gel method using water and their enhanced photocatalytic properties. Korean J Chem Eng 36:2118–2124
68. Meenakshi G, Sivasamy A (2022) Enhanced photocatalytic activities of CeO2@ ZnO core-shell nanostar particles through delayed electron hole recombination process. Colloids Surf A: Physicochem Eng Asp 645:128920
69. Fang J, Fan H, Ma Y, Wang Z, Chang Q (2015) Surface defects control for ZnO nanorods synthesized by quenching and their anti-recombination in photocatalysis. Appl Surf Sci 332:47–54
70. Xu Y, Li H, Sun B, Qiao P, Ren L, Tian G, Zhou W (2020) Surface oxygen vacancy defect-promoted electron–hole separation for porous defective ZnO hexagonal plates and enhanced solar-driven photocatalytic performance. Chem Eng J 379:122295
71. Mirzaeifard Z, Shariatinia Z, Jourshabani M, Rezaei Darvishi SM (2020) ZnO photocatalyst revisited: effective photocatalytic degradation of emerging contaminants using S-doped ZnO nanoparticles under visible light radiation. Ind Eng Chem Res 59(36):15894–15911
72. Saffari R, Shariatinia Z, Jourshabani M (2020) Synthesis and photocatalytic degradation activities of phosphorus containing ZnO microparticles under visible light irradiation for water treatment applications. Environ Pollut 259:113902
73. Choi J, Chan S, Joo H, Yang H, Ko FK (2016) Three-dimensional (3D) palladium-zinc oxide nanowire nanofiber as photo-catalyst for water treatment. Water Res 101:362–369
74. Danwittayakul S, Jaisai M, Dutta J (2015) Efficient solar photocatalytic degradation of textile wastewater using ZnO/ZTO composites. Appl Catal B Environ 163:1–8
75. Lv J, Zhu Q, Zeng Z, Zhang M, Yang J, Zhao M, Sun Z (2017) Enhanced photocurrent and photocatalytic properties of porous ZnO thin film by Ag nanoparticles. J Phys Chem Solids 111:104–109
76. Bhatia S, Verma N (2017) Photocatalytic activity of ZnO nanoparticles with optimization of defects. Mater Res Bull 95:468–476
77. Raj KP, Sadaiyandi K, Kennedy A, Thamizselvi R (2016) Structural, optical, photoluminescence and photocatalytic assessment of Sr-doped ZnO nanoparticles. Mater Chem Phys 183:24–36
78. Pal M, Bera S, Sarkar S, Jana S (2014) Influence of Al doping on microstructural, optical and photocatalytic properties of sol–gel based nanostructured zinc oxide films on glass. RSC Adv 4(23):11552–11563
79. Mittal M, Sharma M, Pandey OP (2014) UV–Visible light induced photocatalytic studies of Cu doped ZnO nanoparticles prepared by co-precipitation method. Sol Energy 110:386–397
80. Yi S, Cui J, Li S, Zhang L, Wang D, Lin Y (2014) Enhanced visible-light photocatalytic activity of Fe/ZnO for rhodamine B degradation and its photogenerated charge transfer properties. Appl Surf Sci 319:230–236
81. Amornpitoksuk P, Suwanboon S, Sangkanu S, Sukhoom A, Muensit N, Baltrusaitis J (2012) Synthesis, characterization, photocatalytic and antibacterial activities of Ag-doped ZnO powders modified with a diblock copolymer. Powder Technol 219:158–164
82. Dhivya A, Yadav R (2022) An Eco-approach synthesis of undoped and Mn doped ZnO nano-photocatalyst for prompt decoloration of methylene blue dye. Mater Today: Proc 48:494–501
83. Ullah R, Dutta J (2008) Photocatalytic degradation of organic dyes with manganese-doped ZnO nanoparticles. J Hazard Mater 156(1-3):194–200
84. Kuriakose S, Satpati B, Mohapatra S (2014) Enhanced photocatalytic activity of Co doped ZnO nanodisks and nanorods prepared by a facile wet chemical method. Phys Chem Chem Phys 16(25):12741–12749
85. Anandan S, Miyauchi M (2011) Ce-doped ZnO (Ce x Zn 1− x O) becomes an efficient visible-light-sensitive photocatalyst by co-catalyst (Cu 2+) grafting. Phys Chem Chem Phys 13(33):14937–14945
86. Sin JC, Lam SM, Satoshi I, Lee KT, Mohamed AR (2014) Sunlight photocatalytic activity enhancement and mechanism of novel europium-doped ZnO hierarchical micro/nanospheres for degradation of phenol. Appl Catal B Environ 148:258–268
87. Macías-Sánchez JJ, Hinojosa-Reyes L, Caballero-Quintero AD, De La Cruz W, Ruiz-Ruiz E, Hernández-Ramírez A, Guzmán-Mar JL (2015) Synthesis of nitrogen-doped ZnO by sol–gel method: characterization and its application on visible photocatalytic degradation of 2, 4-D and picloram herbicides. Photochem Photobiol Sci 14:536–542
88. Samadi M, Shivaee HA, Zanetti M, Pourjavadi A, Moshfegh A (2012) Visible light photocatalytic activity of novel MWCNT-doped ZnO electrospun nanofibers. J Mol Catal A: Chem 359:42–48
89. Deng H, Xu F, Cheng B, Yu J, Ho W (2020) Photocatalytic CO_2 reduction of C/ZnO nanofibers enhanced by an Ni-NiS cocatalyst. Nanoscale 12(13):7206–7213
90. Tuama AN, Abass KH, Agam MAB (2021) Efficiency enhancement of nano structured Cu2O: Ag/laser etched silicon-thin films fabricated via vacuum thermal evaporation technique for solar cell application. Optik 247:167980
91. Ojha DP, Joshi MK, Kim HJ (2017) Photo-Fenton degradation of organic pollutants using a zinc oxide decorated iron oxide/reduced graphene oxide nanocomposite. Ceram Int 43(1):1290–1297
92. Azizi F (2017) Synthesis and characterization of graphene–N-doped TiO 2 nanocomposites by sol–gel method and investigation of photocatalytic activity. J Mater Sci Mater Electron 28:11222–11229
93. Hao R, Wang G, Jiang C, Tang H, Xu Q (2017) In situ hydrothermal synthesis of g-C3N4/TiO2 heterojunction photocatalysts with high specific surface area for Rhodamine B degradation. Appl Surf Sci 411:400–410
94. Boyadjiev SI, Kéri O, Bárdos P, Firkala T, Gáber F, Nagy ZK, Szilágyi IM (2017) TiO2/ZnO and ZnO/TiO2 core/shell nanofibers prepared by electrospinning and atomic layer deposition for photocatalysis and gas sensing. Appl Surf Sci 424:190–197
95. Abarna B, Preethi T, Karunanithi A, Rajarajeswari GR (2016) Influence of jute template on the surface, optical and photocatalytic properties of sol-gel derived mesoporous zinc oxide. Mater Sci Semicond Process 56:243–250
96. Ranjith KS, Manivel P, Rajendrakumar RT, Uyar T (2017) Multifunctional ZnO nanorod-reduced graphene oxide hybrids nanocomposites for effective water remediation: Effective

sunlight driven degradation of organic dyes and rapid heavy metal adsorption. Chem Eng J 325:588–600
97. Song Y, Shao P, Tian J, Shi W, Gao S, Qi J, Cui F (2016) One-step hydrothermal synthesis of ZnO hollow nanospheres uniformly grown on graphene for enhanced photocatalytic performance. Ceram Int 42(1):2074–2078
98. Ranjbari A, Mokhtarani N (2018) Post treatment of composting leachate using ZnO nanoparticles immobilized on moving media. Appl Catal B: Environ 220:211–221
99. Selvam K, Muruganandham M, Muthuvel I, Swaminathan M (2007) The influence of inorganic oxidants and metal ions on semiconductor sensitized photodegradation of 4-fluorophenol. Chem Eng J 128(1):51–57
100. Gaya UI, Abdullah AH, Zainal Z, Hussein MZ (2009) Photocatalytic treatment of 4-chlorophenol in aqueous ZnO suspensions: Intermediates, influence of dosage and inorganic anions. J Hazard Mater 168(1):57–63
101. Nezamzadeh-Ejhieh A, Khodabakhshi-Chermahini F (2014) Incorporated ZnO onto nano clinoptilolite particles as the active centers in the photodegradation of phenylhydrazine. J Ind Eng Chem 20(2):695–704
102. Assi N, Mohammadi A, Sadr Manuchehri Q, Walker RB (2015) Synthesis and characterization of ZnO nanoparticle synthesized by a microwave-assisted combustion method and catalytic activity for the removal of ortho-nitrophenol. Desalin Water Treat 54(7):1939–1948
103. Sobana N, Swaminathan M (2007) The effect of operational parameters on thephotocatalytic degradation of Acid Red 18 by ZnO. Sep Purif Technol 56(1):101e107
104. Xie J, Li Y, Zhao W, Bian L, Wei Y (2011) Simple fabrication and photocatalytic activity of ZnO particles with different morphologies. Powder Technol 207(1-3):140–144
105. Siuleiman S, Kaneva N, Bojinovaa A, Papazova K, Apostolov A, Dimitrov D (2014) Photodegradation of Orange II by ZnO and TiO2 powders and nanowire ZnO and ZnO/TiO2 thin films. Colloids Surf A Physicochem Eng Asp 460:408e413
106. Pare B, Jonnalagadda SB, Tomar H, Singh P, Bhagwat VW (2008) ZnO assisted photocatalytic degradation of acridine orange in aqueous solution using visible irradiation. Desalination 232(1-3):80–90
107. Mai FD, Chen CC, Chen JL, Liu SC (2008) Photodegradation of methyl green using visible irradiation in ZnO suspensions: determination of the reaction pathway and identification of intermediates by a high-performance liquid chromatography–photodiode array-electrospray ionization-mass spectrometry method. J Chromatogr A 1189(1-2):355–365
108. Sampaio MJ, Lima MJ, Baptista DL, Silva AM, Silva CG, Faria JL (2017) Ag-loaded ZnO materials for photocatalytic water treatment. Chem Eng J 318:95–102